

Clustering of Catalytic Nanocompartments for Enhancing an Extracellular Non-Native Cascade Reaction

Viviana Maffei,^{a,b†} Andrea Belluati,^{a†} Ioana Craciun,^a Dalin Wu,^a Samantha Novak,^a Cora-Ann Schoenenberger,^{a,b} Cornelia G. Palivan^{a,b*}

a. Department of Chemistry, University of Basel, Mattenstrasse 24a, BPR 1096, 4058 Basel, Switzerland

b. NCCR-Molecular Systems Engineering, BPR1095, Mattenstrasse 24a, CH-4058 Basel, Switzerland

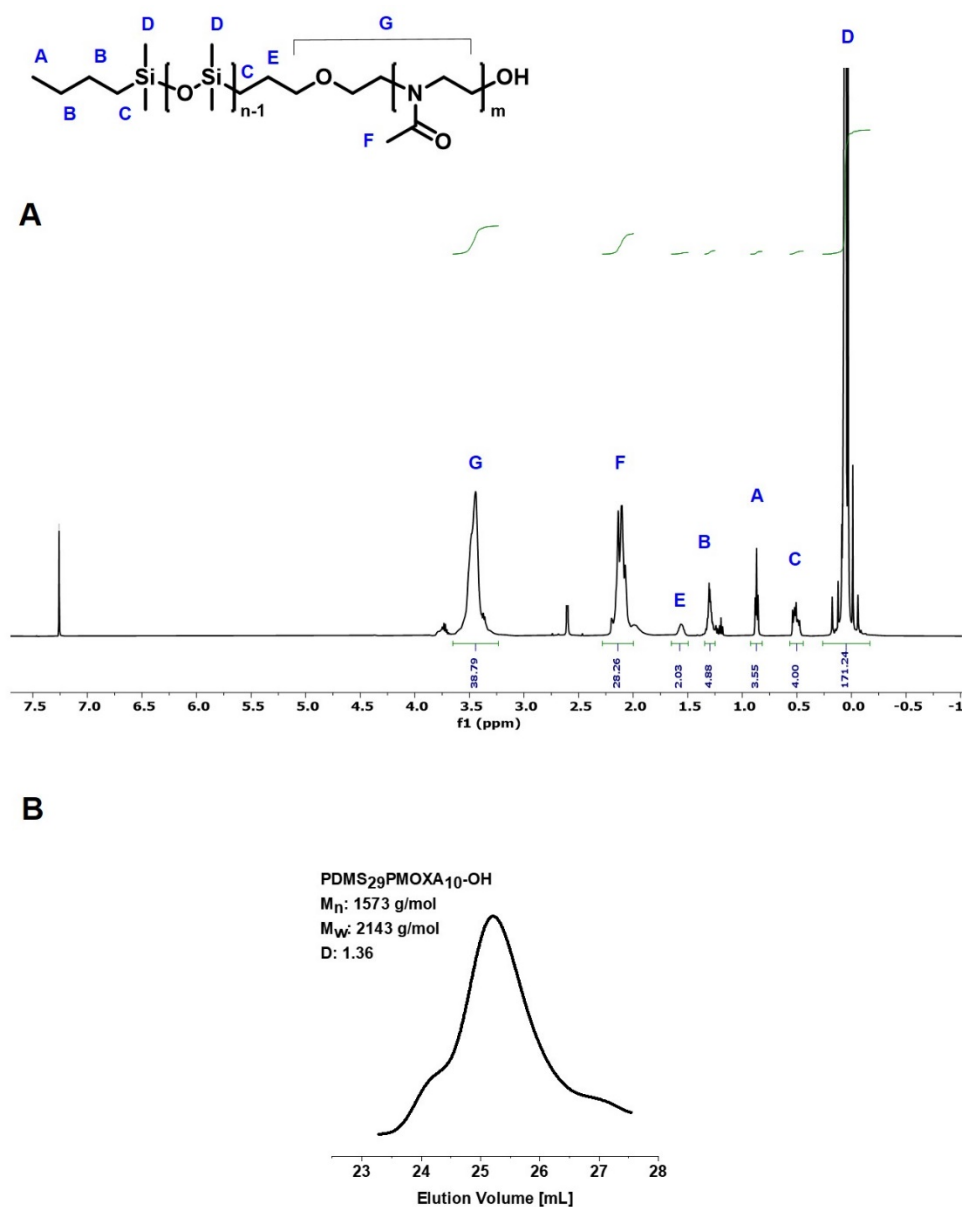


Fig. S1 A ¹H NMR spectra of PDMS₂₉-PMOXA₁₀-OH in CDCl₃ and B its GPC trace in THF.

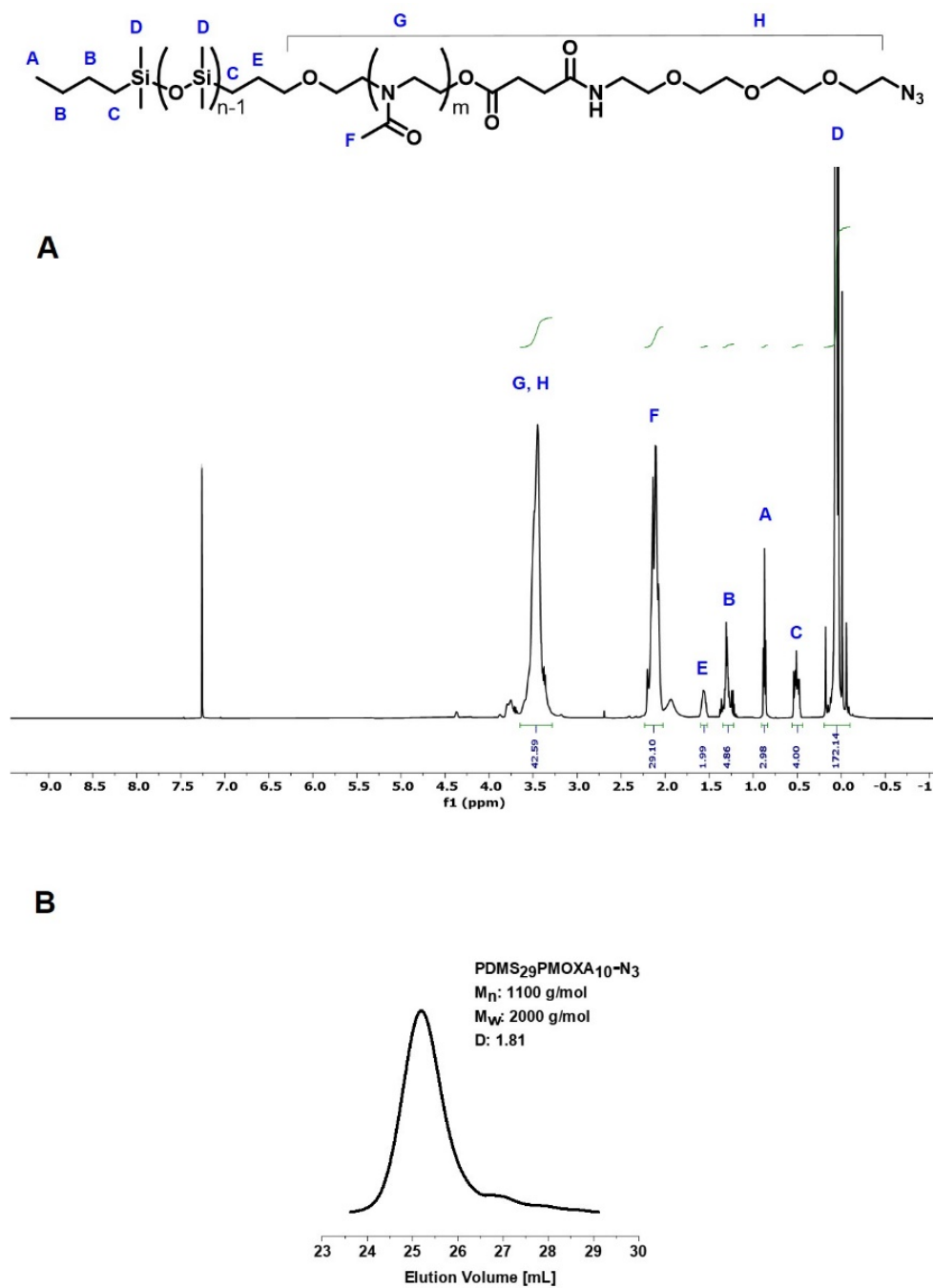


Fig. 2S **A** ¹H NMR spectra of PDMS₂₉-PMOXA₁₀-PEG₄-N₃ in CDCl₃ and **B** its GPC trace in THF.

Table S1 Physical parameters of the azide-functionalized CNCs: size (R_h , hydrodynamic radius and R_g , radius of gyration), ratio R_g/R_h (determining the shape), vesicle concentration and concentration of the encapsulated enzyme.

	GOX-CNC	LPO-CNC
R_h (nm)	119 ± 8	170 ± 24
R_g (nm)	110 ± 2	150 ± 11
R_g/R_h	0.9	0.9
CNC concentration (vesicles/mL)	$1.7 \times 10^{11} \pm 0.1 \times 10^{11}$	$1.2 \times 10^{11} \pm 0.1 \times 10^{11}$
Enzyme concentration ($\mu\text{g/mL}$)	246 ± 23	220 ± 40

Table S2 Quantification of several enzyme- and vesicle-related parameters by FCS. The diffusion time of free dye, free enzyme and encapsulated enzyme are directly correlated to the size of the fluorescent species. The dye/enzyme and enzyme/vesicle ratios are derived from the measurement of brightness intensity per particle for each sample. The percentage of free enzyme is deduced from fitting the measurements of CNCs with a two-component fit: the fast-moving component is assumed to represent unencapsulated enzyme that was not removed by purification, and served for quantification.

	GOX (ATTO 488)	LPO (DyLight 633)
τ free dye (μs)	33 ± 13	81 ± 15
τ enzyme (μs)	249 ± 62	487 ± 154
Dye/enzyme	1 ± 0.2	4 ± 2
τ CNC (μs)	5486 ± 2510	10052 ± 5459
Enzyme/vesicle	11 ± 4	52 ± 32
Free enzyme (%)	2 ± 1	2 ± 1

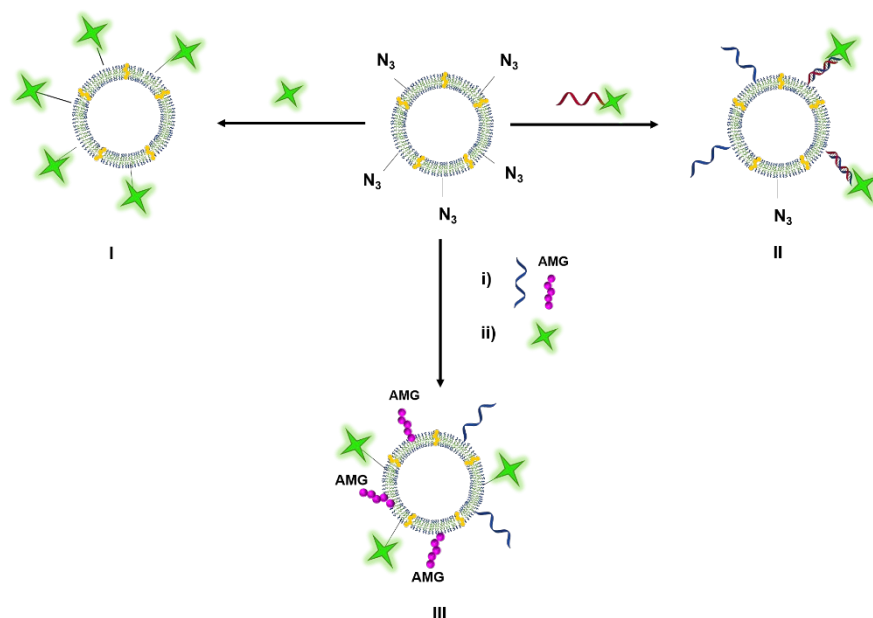


Fig. S3 Labelling strategies used to quantify membrane moieties and conjugated molecules by FCS. I) Polymersomes comprising surface-exposed azides are labelled with Atto488–DBCO (green stars). Measuring the fluorescence intensity per vesicle provides an estimation of how many azides are accessible on the surface of the vesicle. II) Alternatively, ssDNA is conjugated to the vesicle (blue) and then hybridized to an excess of dye-labelled complementary ssDNA (red), e.g., fluorescent 11T-22b base-paired to 11T-22a, which allows the DNA strands per vesicle to be calculated. III) The third strategy involves conjugating 11T-22a to the polymersome at subsaturating concentrations. Subsequently, DBCO-PEG-AMG is conjugated to remaining, non-derivatized azides. Finally, the last available azides are derivatized with Atto488-DBCO. Knowing how many N_3 were originally accessible, and how many DNA strands can be conjugated on average to a vesicle, the coupled AMG molecules can be calculated.

Table S3 Quantification of accessible N_3 , DNA strands and AMG on the vesicle surface by FCS. The total AMG concentration was determined by measuring the absorbance at 280nm. The number of attached 11T-22b and 11T-22a ssDNA was quite broadly distributed which did not affect with cluster formation.

N_3 /vesicle	104 ± 24	
	11T-22a (22b-Atto488)	11T-22b (22a-Cy5)
DNA/vesicle	69 ± 64	34 ± 28
AMG/vesicle	35 ± 4	-
AMG (µg/mL)	1000	

Table S4 Single-stranded DNA used in this study

Strand code	Sequence	Conjugated to CNC
11T-22a	DBCO-5'-TTT TTT TTT TTC CTC GTC CTG CTA ATC CTG TTA-3'	GOX-CNC
11T-22b	DBCO-5'-TTT TTT TTT TTT AAC AGG ATT AGC AGA GCG AGG-3'	LPO-CNC

The calculation of inter-vesicle distance in presence of a cascade reaction

$$\langle D \rangle = d \left[\xi \left(\frac{\pi}{6\phi} \right)^{\frac{1}{3}} e^{(1.5 \ln^2 \sigma)} - e^{(0.5 \ln^2 \sigma)} \right]$$

Equation 1

According to the previously-developed equation, the mean inter-vesicle distance (D) depends on: the mean size of vesicles d ; the spatial distribution parameter ξ (fixed to 1.1¹ for well-dispersed systems), which is a measure of the dispersion –mixing– of the colloidal system; the volume fraction occupied by vesicles ϕ ; and the geometric standard deviation σ .

From the literature,¹ ϕ can be approximated in the case of vesicles, to the general equation.

$$\phi = N \times V$$

Equation 2

For our system, however, not all vesicles were equal, as the “bridging molecule”, H₂O₂, could only go productively from a GOX- to an LPO-CNC (as a GOX-to-GOX diffusion essentially means travelling through empty space), and we had to consider both their relative concentrations and sizes. The ratios between the d and ϕ (relative size and frequency, respectively) of GOX- and LPO CNCs, i.e. the probability of hydrogen peroxide to encounter the right CNC once diffused out of GOX-CNC, yielded the weighted value

$$W_d = \frac{d_{LPO}}{d_{GOX}}$$

Equation 3

Which represents the probability of a molecule to encounter an LPO-CNC: bigger vesicles will mean a higher probability of H₂O₂ finding its way to the enzyme, and vice-versa. Similarly,

$$W_\phi = \frac{\phi_{LPO}}{\phi_{GOX}}$$

Equation 4

H₂O₂ will more likely travel to the adequate CNC if its concentration is higher.

From Equation 3 and Equation 4 we can derive the overall equation for the contributions of the CNCs populations.

$$\langle D \rangle = d_{LPO} W_d \left[\xi \left(\frac{\pi}{6\phi_{LPO} W_\phi} \right)^{\frac{1}{3}} e^{(1.5 \ln^2 \sigma_{LPO})} - e^{(0.5 \ln^2 \sigma_{LPO})} \right] \\ + d_{GOX} (1 - W_d) \left[\xi \left(\frac{\pi}{6\phi_{GOX} (1 - W_\phi)} \right)^{\frac{1}{3}} e^{(1.5 \ln^2 \sigma_{GOX})} - e^{(0.5 \ln^2 \sigma_{GOX})} \right]$$

Equation 5

However, the necessity of Equation 5 ends in the moment of clustered CNCs: as the inter-vesicle distance within the cluster is negligible compared to that between clusters, the clusters themselves can be considered as a single entity. This does not exclude the diffusion between cluster (for which Equation 1 is sufficient), nor does clustering annul the influence of diffusion across membranes on the reaction efficiency.²

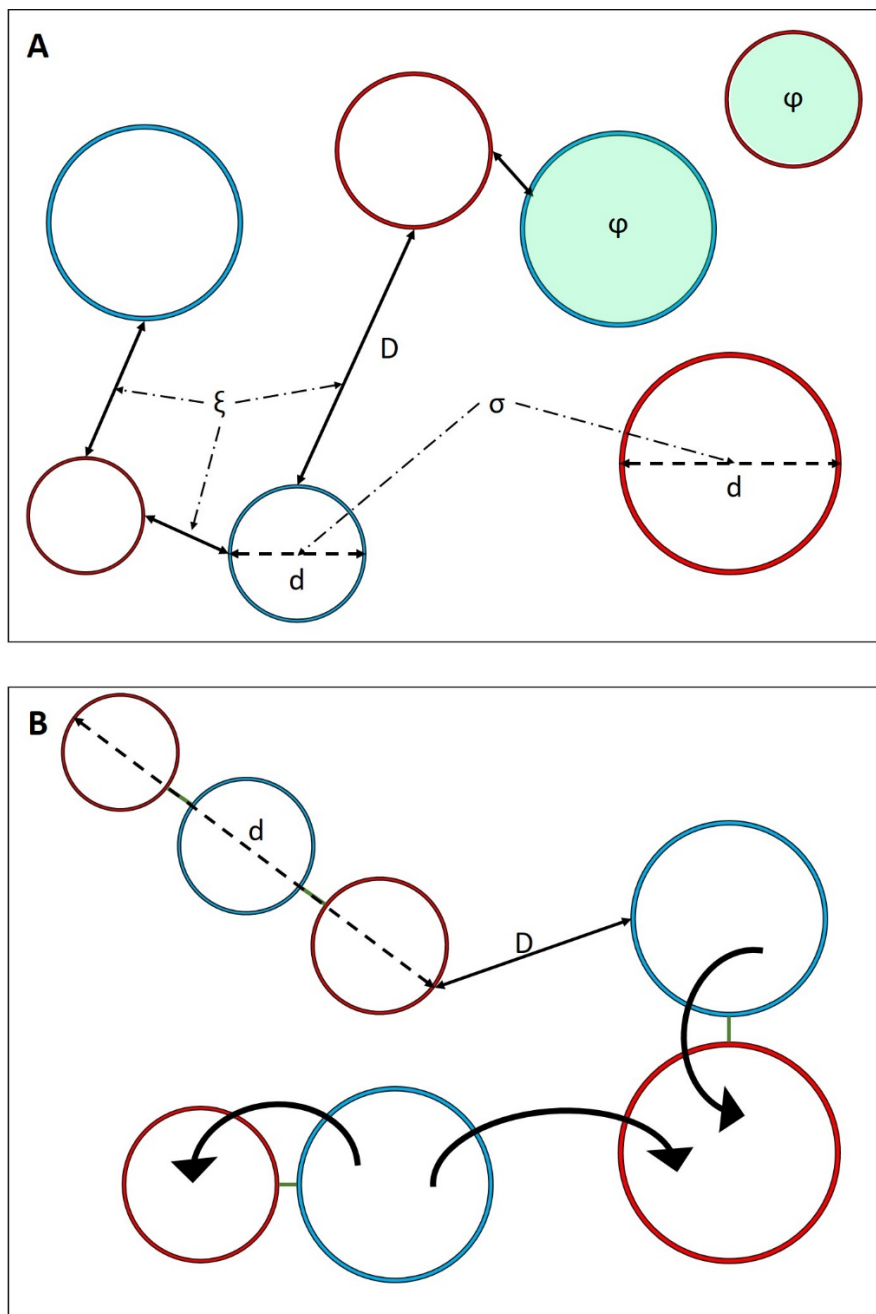


Fig. S4 A. Schematic representation of the equation derived to determine mean inter-vesicle/inter-cluster distance (D). In a well-dispersed sample, D depends on the mean particle size d , their size distribution (standard deviation σ), on the total sample volume occupied by the vesicles (φ), and the spatial distribution parameter (ξ). Compared however to the original equation ¹, not all vesicles are assumed equal, as only the diffusion between the first to the second CNC in a cascade (e.g. blue to red) is a “fruitful” movement, so this was taken into account. B. This 2-population assumption, however, is no longer necessary for a clustered system, as now the bridging molecule of the cascade is easily channelled from blue to red thanks to a constant distance. The inter-cluster diffusion is still possible, but less likely. Now the sizes are those of the whole cluster, rather than the single vesicles.

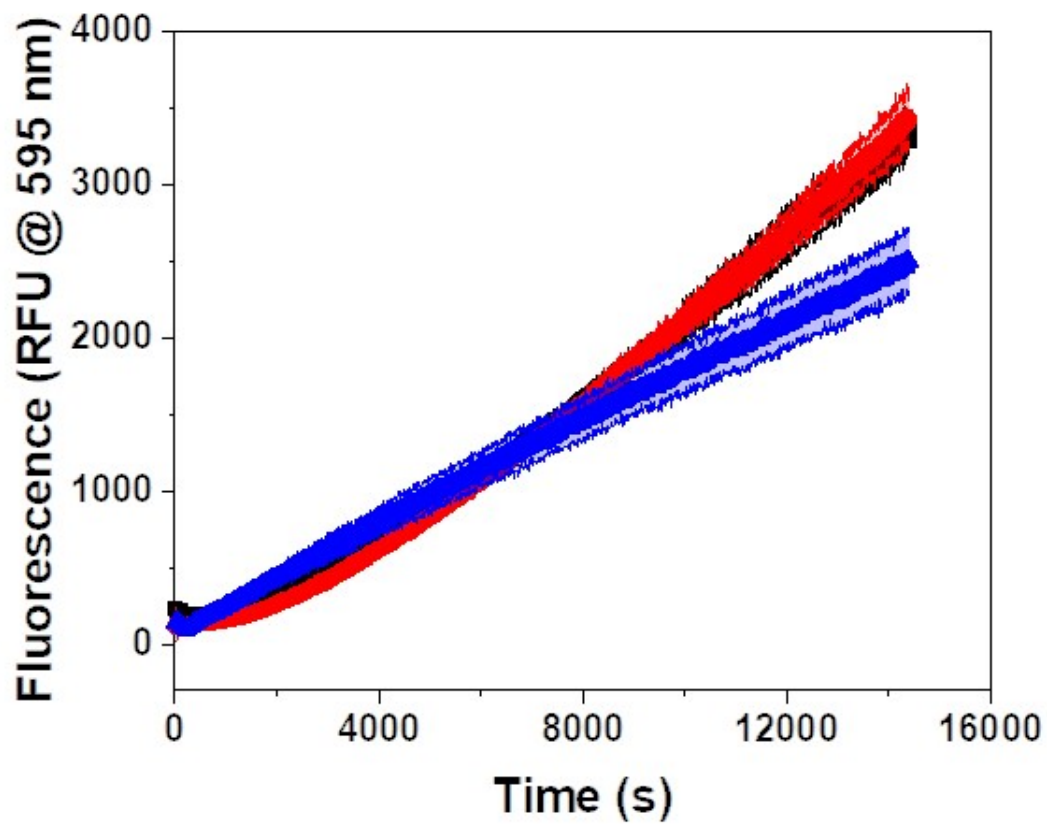


Fig. S5 Activity of AMG in clusters showing a full cascade dependence on AMG activity even in the presence of additional glucose in solution. Blue: AMG(GOX)-LPO cluster activity in the presence of glucose. Red: AMG(GOX)-LPO activity in the presence of amylose. Black: AMG(GOX)-LPO activity in the presence of amylose and extra glucose.

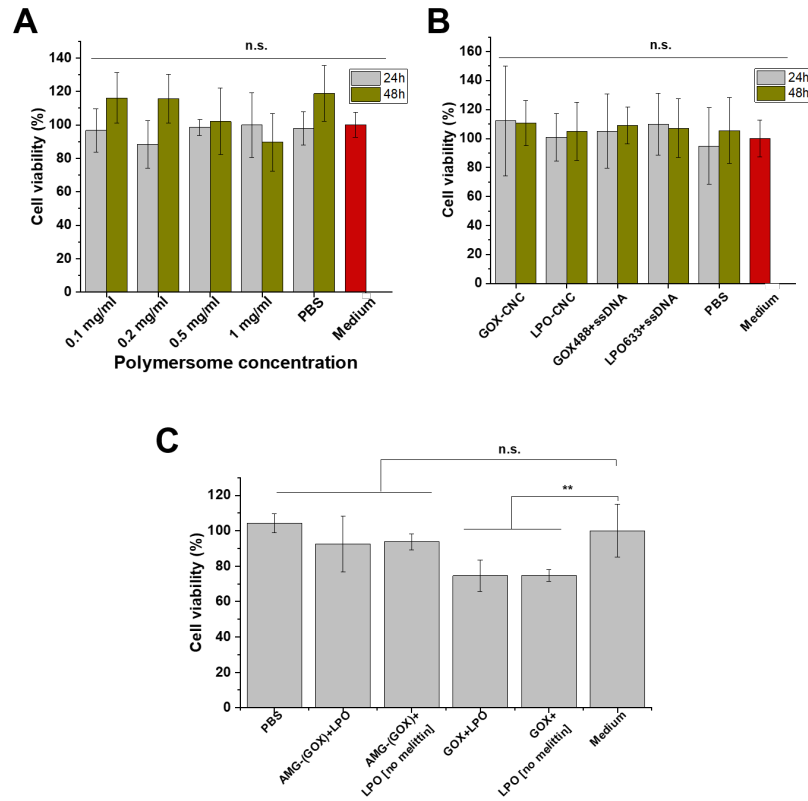


Fig. S6 MTS proliferation assay of A. Cells exposed to empty polymersomes at different concentrations. B. Cells exposed to 0.2 mg/mL of CNCs, CNCs with ssDNA, and PBS compared to culture medium. No significant difference ($p > 0.05$) in cell proliferation was detected, meaning that at this concentration the non-clustered CNCs were not found to have any effect on cell viability. C. Cells exposed to clusters. Clusters with GOX-CNCs showed a low, but significant decrease in viability (**, $p < 0.1$), unless they were decorated with AMG, which apparently slowed down the rate of H_2O_2 production.

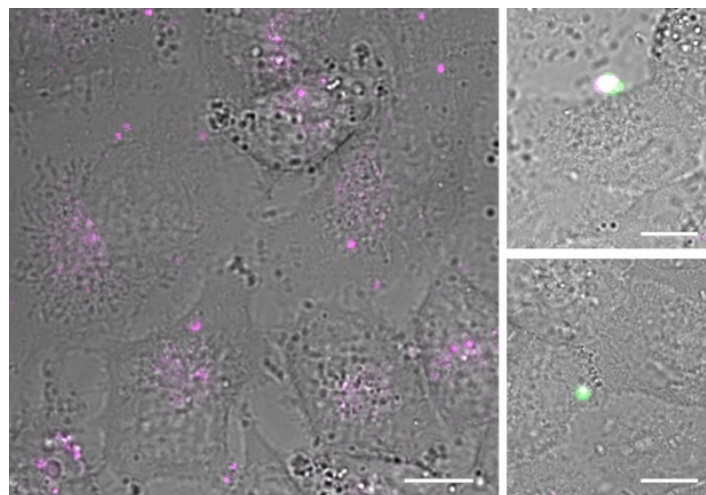


Fig. S7 Merged brightfield and fluorescence CLSM images showing clustered CNCs (Atto-488-GOX/Dy633-LPO) on A549 cells. Scale bars, 10 μ m.

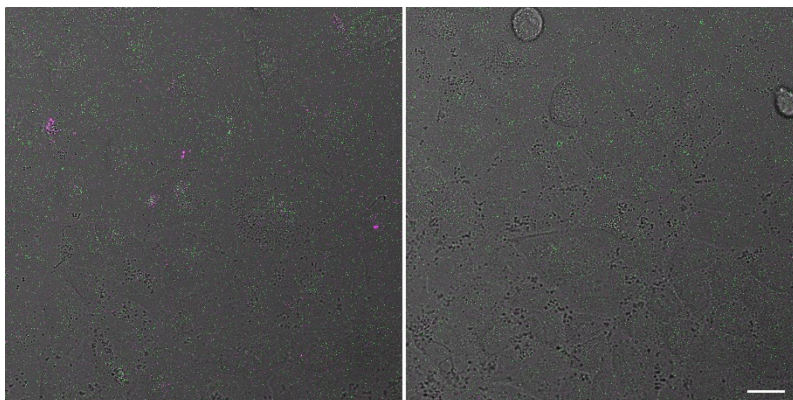


Fig. S8 Merged brightfield and fluorescence CLSM images showing non-clustered CNCs (Atto-488-polymersomes and Dy633-polymersomes) on A549 cells on the left and untreated A549 cells on the right. Scale bar, 20 μ m.

Table S5 Colocalization analysis of non-clustered and clustered CNCs according to Pearson's and Manders' coefficient. The Costes P-value indicates whether colocalization/anticolocalization is statistically significant, with 1 being significant and 0 non-significant.

	CNCs	Clustered CNCs
Pearson's coefficient	-0.73	0.27
Manders' tM1	0.064	0.144
Costes P-Value	0	1

References

1. Z. H. Liu, Y. Li and K. W. Kowk, *Polymer*, 2001, **42**, 2701-2706.
2. A. Belluati, I. Craciun, J. Liu and C. G. Palivan, *Biomacromolecules*, 2018, DOI: 10.1021/acs.biomac.8b01019.